Taylor & Francis
Taylor & Francis Group

New information on postcranial skeleton of the Early Cretaceous Gansus yumenensis (Aves: Ornithuromorpha)

Ya-Ming Wang, Jingmai K. O'Connor, Da-Qing Li & Hai-Lu You

Taylor & Francis
Taylor & Francis Group

New information on postcranial skeleton of the Early Cretaceous *Gansus yumenensis* (Aves: Ornithuromorpha)

Ya-Ming Wang[a,b]*, Jingmai K. O'Connor[b,c], Da-Qing Li[d] and Hai-Lu You[b,c]

[a]*School of Earth Sciences and Resources, China University of Geosciences (Beijing), Beijing 100083, P.R. China;* [b]*Key Laboratory of Vertebrate Evolution and Human Origins of Chinese Academy of Sciences, Beijing 100044, P.R. China;* [c]*Institute of Vertebrate Paleontology and Paleoanthropology, Chinese Academy of Sciences, Beijing 100044, P.R. China;* [d]*Gansu Geological Museum, Lanzhou, Gansu Province 730010, P.R. China*

Gansus yumenensis Hou and Liu, 1984 is a basal ornithuromorph bird that has been recovered from the Lower Cretaceous Xiagou Formation in the Changma Basin of Gansu Province in northwestern China. Although it bears important significance in understanding the origin and early evolution of Ornithuromorpha, this taxon has only received preliminary morphological study. Here, we provide a detailed description of the postcranial morphology of *Gansus yumenensis* based on seven new specimens and new data from previously reported specimens, and update diagnosis for this taxon. Our phylogenetic analysis including new morphological data on *Gansus yumenensis* resolves all known four genera of Changma ornithuromorphs as more derived taxa than Jehol members of this clade, indicating the difference between Changma and Jehol avifauna.

Keywords: *Gansus yumenensis*; Changma; Xiagou Formation; Early Cretaceous; Ornithuromorpha; anatomy; phylogeny

Introduction

Gansus yumenensis Hou and Liu, 1984 was named based on an isolated left foot (IVPP V6862) collected from the Lower Cretaceous Xiagou Formation in the Changma Basin of Gansu Province in northwestern China. At the time of its discovery, this specimen represented the first Mesozoic fossil bird from China and the second oldest bird in the world, younger only than *Archaeopteryx* (Hou and Liu 1984). Renewed field efforts in the Changma Basin nearly two decades later produced a wealth of far more complete specimens and You et al. (2006) reported five specimens among them (CAGS-IG-04-CM-001 ∼ 004, -008), describing *Gansus yumenensis* as 'a nearly modern amphibious bird'. Their phylogenetic analysis resolved this taxon as a basal member of Ornithurae. Li et al. (2011) provided additional information on the morphology of the sternum, forelimb and hind limb based on nine fragmentary new specimens (IVPP V15074–15077, 15079–15081, 15083, 15084). In addition to *Gansus*, three other ornithuromorph taxa: *Yumenornis huangi*, *Changmaornis houi* and *Jiuquanornis niui* (Wang et al. 2013), one enantiornithine *Qiliania graffini* (Ji et al. 2011) and three unnamed enantiornithine specimens (You et al. 2005; Harris et al. 2006; Lamanna et al. 2006) have also been described from the same locality. However, the vast majority of Changma avian specimens are referred to *Gansus*.

Here we describe seven new specimens of *Gansus yumenensis* (GSGM-07-CM-009, -07-CM-011, -06-CM-

011, -07-CM-006, -05-CM-014, -04-CM-018 and -04-CM-031), all from the Changma locality. We also describe some details of two specimens (CAGS-IG-04-CM-003, -004) reported in You et al. (2006). They together provide a rare opportunity to study the detailed postcranial anatomy of basal ornithuromorphs. Notably, three of the new specimens preserve gastroliths, contributing new information about the habit of *Gansus yumenensis*.

Institutional abbreviations

CAGS-IG, Chinese Academy of Geological Sciences, Institute of Geology, Beijing; **GSGM**, Gansu Geological Museum, Lanzhou; **IVPP**, Institute of Vertebrate Paleontology and Paleoanthropology, Beijing.

Systematic paleontology

Aves Linnaeus, 1758
Pygostylia Chiappe, 2002
Ornithothoraces Chiappe and Calvo, 1994
Ornithuromorpha Chiappe, 2002
Gansus yumenensis Hou and Liu, 1984

Holotype specimen

Distal left tibiotarsus and left tarsometatarsus with complete pedal digits (IVPP V6862; Hou and Liu 1984).

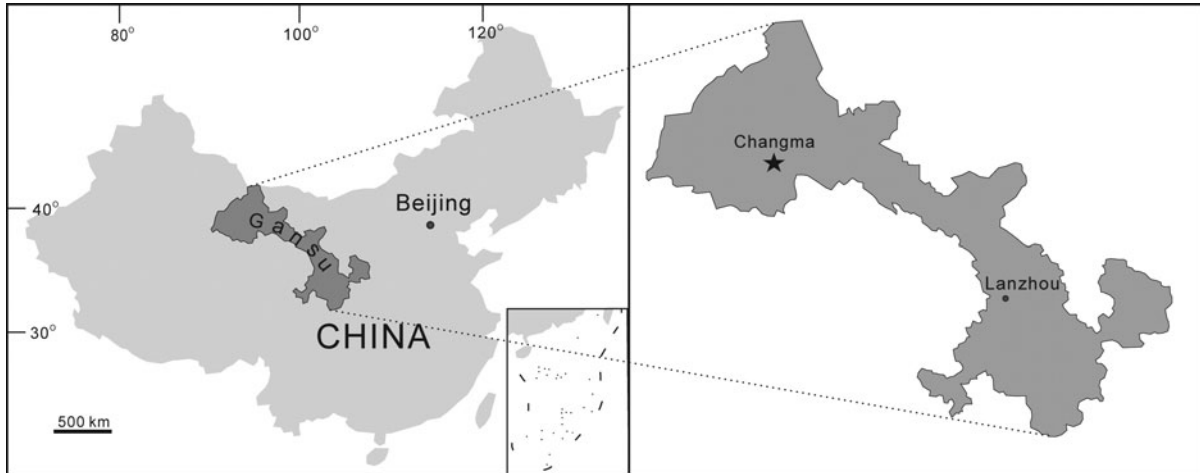*Corresponding author. Email: yaming21@hotmail.com

Figure 1. Geographic location of the Changma Basin (indicated by star), Gansu Province, People's Republic of China. Source: Modified from Wang et al. (2013).

New referred specimens

GSGM-07-CM-009, articulated three caudalmost thoracic vertebrae, synsacrum, pygostyle and partial pelvic girdle consisting of right ilium, proximal pubis and ischium (Figure 2); GSGM-07-CM-011, articulated skeleton and gastroliths, lacking the skull, cervical and caudal vertebrae, pectoral girdles and forelimbs (Figure 3); GSGM-06-CM-011, nearly complete sternum, sternal ribs, partial furcula, sternal ribs and gastroliths (Figure 6); GSGM-07-CM-006, left proximal scapula, coracoid and partial left forelimb, with feather impression (Figure 7); GSGM-05-CM-014, complete left and partial right forelimbs, complete hind limbs, scattered ribs and gastroliths (Figure 8); GSGM-04-CM-018, articulated left tibiotarsus and fibula (Figure 9); GSGM-04-CM-031, proximal and distal portions of left tarsometatarsus (Figure 10).

Locality and horizon

In the vicinity of the Changma Township, Yumen City, Jiuquan area, Gansu Province, northwestern China; Lower Cretaceous (early Aptian), Xiagou Formation (You et al. 2005; Harris et al. 2006; Lamanna et al. 2006; Suarez et al. 2013; Figure 1).

Revised diagnosis

Gansus yumenensis is distinguished from other known ornithuromorphs by the following unique combination of characters: pygostyle narrow throughout length with dorsal spinous ridge; sternum with well-developed craniolateral and lateral processes; lateral trabeculae of sternum curved medially; sternum bearing a pair of caudal fenestrae; coracoid with a cranially hooked lateral process; tibiotarsus long, with two strongly proximally projected cnemial crests; position of metatarsal II trochlea high and plantarly displaced relative to the metatarsal III trochlea; pedal digit IV longest (autapomorphy); pedal claws with pointed flexor tubercles.

Description

Anatomical nomenclature primarily follows Baumel and Witmer (1993). English translations are used for osteological terminology while Latin is maintained for muscles.
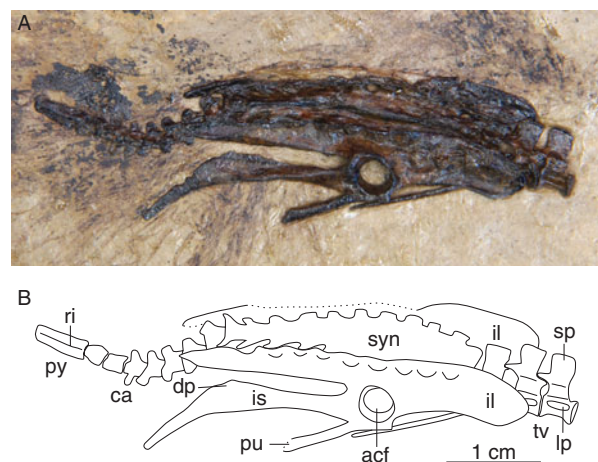

Figure 2. (Colour online) Photograph (A) and line drawing (B) of *Gansus yumenensis* GSGM-07-CM-009. Abbreviations: acf, acetabulum foramen; ca, caudal vertebrae; dp, dorsal process; il, ilium; is, ischium; lp, lateral depression; pu, pubis; py, pygostyle; ri, ridge; sp, spinous process; syn, synsacrum; tv, thoracic vertebrae.

Vertebral column and ribs

GSGM-07-CM-009 preserves the caudalmost three thoracic vertebrae in lateral view and GSGM-07-CM-011 preserves two isolated thoracic vertebrae in caudal view. The thoracic vertebrae possess well-developed rectangular spinous processes, the dorsoventral height of which is nearly half the total height of the associated vertebra (Figure 2). The transverse processes are long and robust (CAGS-IG-04-CM-004; You et al. 2006). The vertebral foramen is large, nearly the same size as the articular surface of the centrum (Figure 3). The length of the centrum is markedly greater than the midpoint width (Figure 2). The thoracic vertebrae appear to be amphicoelous. Like enantiornithines, the lateral depressions on the centra are developed as elongated grooves rather than broad fossae as in other ornithuromorphs (Figure 2).

Based on the number of transverse processes, the synsacrum is composed of ten fully fused vertebrae (Figure 2), as in *Apsaravis* and *Ichthyornis* (Clarke and Norell 2002; Clarke 2004); whereas the synsacrum is formed by nine vertebrae in *Yanornis* and *Yixianornis* (Zhou and Zhang 2001; Clarke et al. 2006), nine or ten in *Jianchangornis* (Zhou et al. 2009), 11 in *Changmaornis* (Wang et al. 2013) and only seven in the basal *Archaeorhynchus* (possibly due to ontogenetic variation) (Zhou and Zhang 2006; Zhou et al. 2013).

The caudal series consists of seven free vertebrae, the cranial five of which possess robust transverse processes; the processes become increasingly slender distally (Figure 2). The pygostyle is short, slightly tapering to the end; its length is approximately equal to the combined length of three free caudal vertebrae, as in CAGS-IG-04-CM-002 (You et al. 2006). The pygostyle is narrow throughout its length and bears a spinous ridge along the dorsal surface (Figure 2), whereas the pygostyle is much fatter proximally in most other basal ornithuromorphs
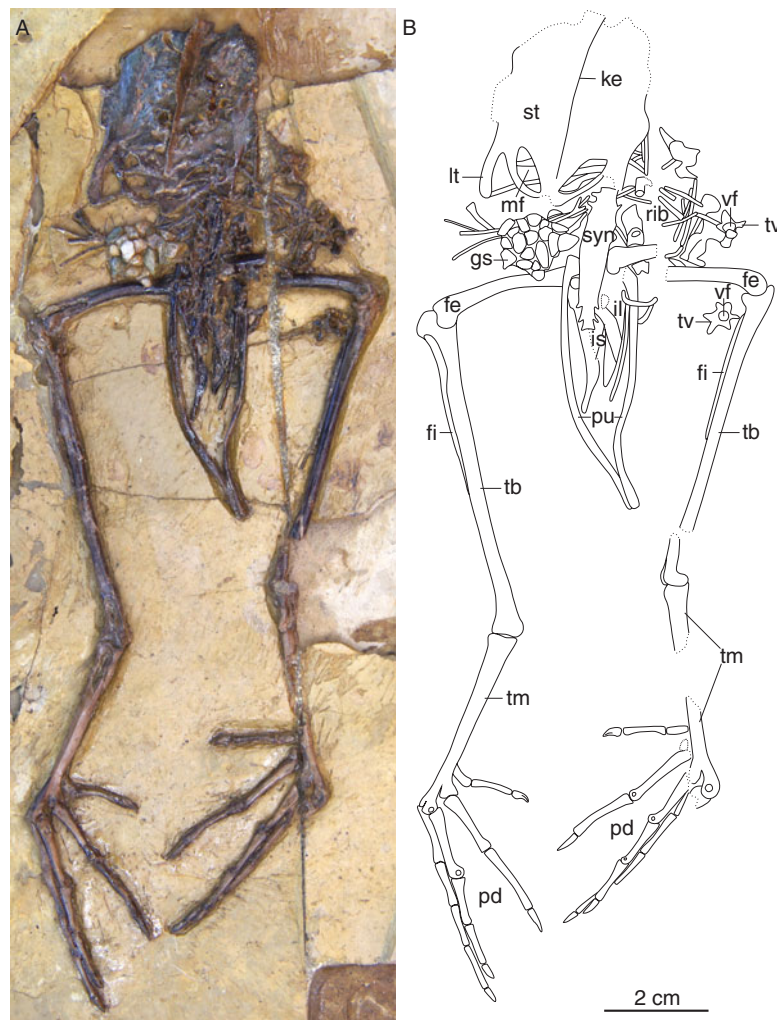

Figure 3. (Colour online) Photograph (A) and line drawing (B) of *Gansus yumenensis* GSGM-07-CM-011. Abbreviations: fe, femur; fi, fibula; gs, gastroliths; il, ilium; is, ischium; ke, keel; lt, lateral trabecula; mf, medial fenestra; pd, pedal digits; pu, pubis; rib, ribs; st, sternum; syn, synsacrum; tb, tibiotarsus; tm, tarsometatarsus; tv, thoracic vertebrae; vf, vertebral foramen.
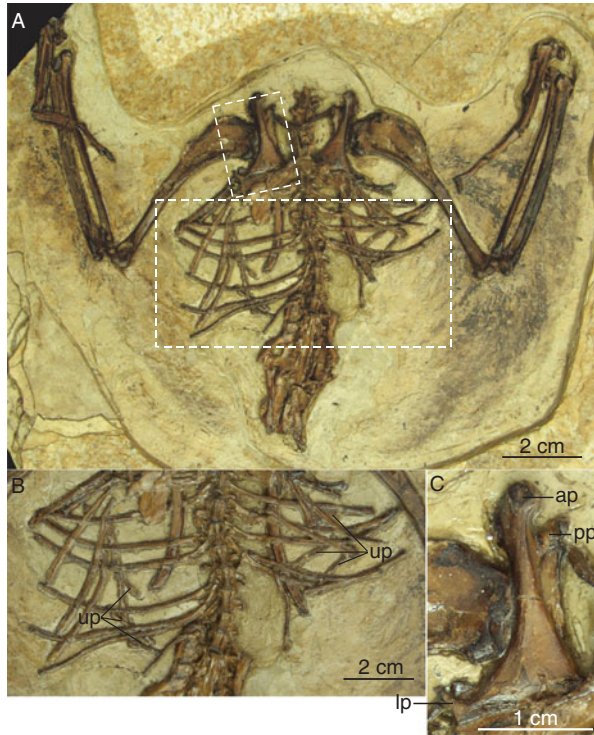
Figure 4. (Colour online) Photograph (A), detail of the ribs (B) and detail of the coracoid of *Gansus yumenensis* CAGS-IG-04-CM-004 (You et al. 2006). Abbreviations: ap, acrocoracoid process; lp, lateral process; pp, procoracoid process; up, uncinated processes.

(e.g., *Yixianornis, Yanornis, Archaeorhynchus*). The total length of the caudal vertebrae and the pygostyle is more than half the length of the synsacrum (Figure 2).

The thoracic ribs are slender, slightly curved and relatively elongate. Six uncinate processes are preserved in CAGS-IG-04-CM-004 (Figure 4(B)), contrary to You et al. (2006); they are elongated and slender, nearly crossing two ribs. At least one of the uncinate processes is in articulation with the rib, but their scattered positions in the fossil suggest that they were not fused to the ribs. The preserved sternal ribs are straight, short and slender; four articulate with the left margin of the sternum, but poor preservation prevents determining the exact number of the sternal ribs (Figure 6). No gastralia is preserved in any specimen, although this element is present in some Jehol ornithuromorphs, such as *Archaeorhynchus*, *Piscivoravis*, *Iteravis* and the recently reported new species of *Gansus*, *Gansus zheni* (Zhou et al. 2013; Liu et al. 2014; Zhou, O'Connor, et al. 2014; Zhou, Zhou, et al. 2014).

Pectoral girdle

The furcula is delicate, U-shaped and lacks a hypocleidium (Figure 5(B); You et al. 2006). This morphology is characteristic of most basal ornithuromorphs. The furcula

Figure 5. (Colour online) Photograph (A) and detail of the furcula of CAGS-IG-04-CM-003 (You et al. 2006). Abbreviation: fu, furcula.

has an intraclavicular angle of approximately 38° (You et al. 2006), similar to *Jiuquanornis* (Wang et al. 2013), but lower than that of *Yixianornis*, *Archaeorhynchus*, *Piscivoravis*, *Iteravis* and *Gansus zheni* (Clarke et al. 2006; Zhou et al. 2013; Liu et al. 2014; Zhou, O'Connor, et al. 2014; Zhou, Zhou, et al. 2014). The Jehol ornithuromorph *Schizooura* possesses a robust V-shaped furcula with a short hypocleidium, being reminiscent of the enantiornithine condition (Zhou et al. 2012). The rami are oval in cross-section at mid-shaft and taper to the omal ends respectively (Figure 5(B); You et al. 2006), lacking epicleidial processes like those present in *Yixianornis*.

In CAGS-IG-04-CM-003 and -004 (Figures 4 and 5; You et al. 2006), the acrocoracoid process on the coracoid is mediolaterally expanded, sub-rounded and slightly hooked medially, with a shallow ligamental groove present ventrally. The well-developed procoracoid process projects medioventrally; its distal tip projects ventrally and is expanded into a small tubercle (Figure 4(C); You et al. 2006). The ventral surface of the shaft of the coracoid is convex. Distally, the sternal margin is straight; the strongly concave lateral margin of the coracoid is longer than the medial margin (Figure 4(C); You et al. 2006),
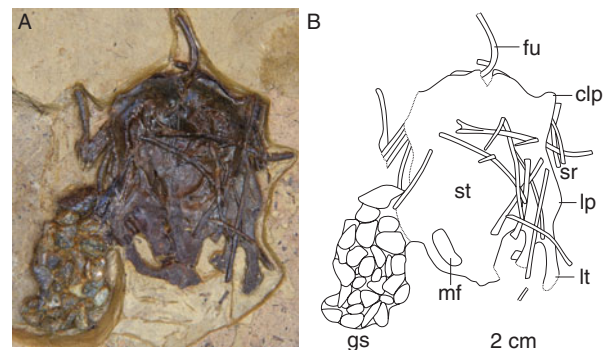

Figure 6. (Colour online) Photograph (A) and line drawing (B) of *Gansus yumenensis* GSGM-06-CM-011. Abbreviations: clp, craniolateral process; fu, furcula; gs, gastroliths; lp, lateral process; lt, lateral trabecula; mf, medial fenestra; sr, sternal ribs; st, sternum.

whereas in *Yumenornis*, *Yanornis* and *Yixianornis*, the two margins are nearly the same in length (Zhou and Zhang 2001; Clarke et al. 2006; Wang et al. 2013). A lateral process is present as a distinct cranially hooked projection (Figure 4(C); You et al. 2006), more projected than in *Gansus zheni* and similar to some neornithines (e.g., *Puffinus*); however, this lateral process is absent in other Jehol ornithuromorphs. The left coracoid is exposed dorsally in GSGM-07-CM-006. The deep and circular scapular cotyla on the dorsal surface of the coracoid (Figure 7) resembles that of *Ichthyornis* (Clarke 2004). The n. supracoracoideus foramen is absent, indicating this nerve ran medial to the coracoid. The oval glenoid facet is poorly concave and nearly twice as large as the scapular cotyla. Caudally, the m. sternocoracoidei impression is
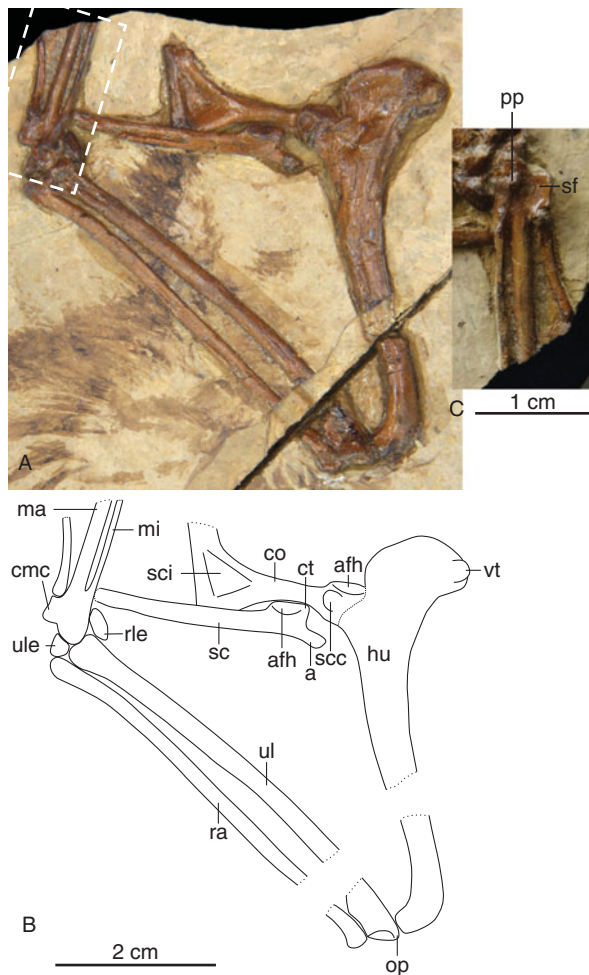

Figure 7.   (Colour online) Photograph (A), line drawing (B) and detail of the carpometacarpus (C) of *Gansus yumenensis* GSGM-07-CM-006. Abbreviations: a, acromion; afh, articular surface with humerus; cmc, carpometacarpus; co, coracoid; ct, coracoidal tubercle; hu, humerus; ma, major metacarpal; mi, minor metacarpal; op, olecranon process; pp, pisiform process; ra, radius; rle, radiale; sc, scapula; scc, scapular cotyla; sci, sternocoracoidei m. impression; sf, supratrochlear fossa; ul, ulna; ule, ulnare; vt, ventral tubercle.

shallow and sub-triangular, similar to that in *Yixianornis* and other ornithuromorphs (Figure 7).

The proximal end of the left scapula is preserved in lateral view in GSGM-07-CM-006. The acromion process of the scapula is long, extending far beyond the coracoidal tubercle (Figure 7); whereas in *Yumenornis*, *Yixianornis* and *Archaeorhynchus*, the acromion process extends only slightly past the coracoidal tubercle and in *Ichthyornis* not at all (Clarke 2004; Clarke et al. 2006; Zhou and Zhang 2006; Wang et al. 2013). A mediolaterally compressed articular surface for the furcula is developed on the acromion. The coracoidal tubercle is small, sub-rounded and confluent with the glenoid facet (the articular surface for the humerus), which is large and shallowly concave. A deep sulcus is present on the surface of the scapular shaft (Figure 7), also present in *Ambiortus* (Kurochkin 1982; O'Connor and Zelenkov 2013).

The sternum is preserved in dorsal view in GSGM-06-CM-011 and in ventral view in GSGM-07-CM-011. Cranially, the sulci for the articulation of the coracoid are well developed, but their exact depth cannot be determined. The rostral margin of the sternum is rounded, defining an angle of approximately 140° (Figure 6), contrasting to the 'peaked' rostral margin in *Jianchangornis*, *Yixianornis*, *Yanornis*, *Songlingornis*, *Yumenornis* and *Iteravis* (Hou 1997; O'Connor and Zhou 2013; Wang et al. 2013; Zhou, O'Connor, et al. 2014). The craniolateral processes are deflected dorsolaterally, defining an obtuse angle of approximately 100°, greater than that in *Yanornis*, *Songlingornis* and *Yumenornis*. The lateral (zyphoid) process (Clarke et al. 2006) is a craniocaudally elongated rectangular process with weakly rounded craniolateral and caudolateral margins; the process is mediolaterally narrower than that in *Yumenornis*, *Yixianornis* and *Iteravis*. A dorsoventrally high keel extends from the rostral margin nearly to the caudal terminus of the sternum, also visible in CAGS-IG-04-CM-003 (Figures 3 and 5(A); You et al. 2006). The height of the keel is greatest at the rostral end and decreases distally, and the rostroventral tip of the keel is located proximal to the rostral margin of the sternal corpus (Figure 3), as in IVPP V15076 (Li et al. 2011). Caudally, the lateral trabecula is short, strap-like and weakly curved medially, without a caudal expansion like that present in many other ornithuromorphs, such as *Yanornis*, *Yixianornis* and *Songlingornis* (Figure 3). The medially curved lateral trabecula is contrary to the laterally oriented lateral trabecula of IVPP V15076 described in Li et al. (2011); this difference is possibly due to the broken distal end of the lateral trabecula in IVPP V15076. The intermediate trabecula is more slender than the lateral one, and fused to the xiphial region, forming an enclosed caudal fenestra (Figure 6), as in *Yanornis*, *Yixianornis* and *Songlingornis*; the fenestrae are much smaller in *Yanornis* and *Songlingornis*, and rounder in *Yixianornis* (Hou 1997; Zhou and Zhang 2001; Clarke et al. 2006).

Forelimb

The humeri are exposed in caudal view in both GSGM-07-CM-006 and GSGM-05-CM-014 (Figures 7 and 8). The ventral tubercle is proximoventrally developed,

resembling that of *Yumenornis*, *Yixianornis*, *Yanornis* and *Longicrusavis* (Zhou and Zhang 2001; Clarke et al. 2006; O'Connor et al. 2010; Wang et al. 2013), and bears a shallow fossa on its dorsal surface (Figure 7); this fossa is

Figure 8. (Colour online) Photograph (A), line drawing (B) and detail of the distal end of the tibiotarsus (C) of *Gansus yumenensis* GSGM-05-CM-014. Abbreviations: bt, bicipital tubercle; cc, cnemial crest; cmc, carpometacarpus; fe, femur; gs, gastroliths; hu, humerus; lc, lateral condyle; ma, major metacarpal; ma I, the first phalanx of the major digit; mc, medial condyle; md, manual digits; mi, minor metacarpal; mi I, the first phalanx of the minor digit; pd, pedal digits; ra, radius; rib, ribs; rle, radiale; tb, tibiotarsus; tm, tarsometatarsus; tu, tubercles; ul, ulna; ule, ulnare; vt, ventral tubercle.

also present in *Ichthyornis*, which is interpreted as muscular insertion that may be related to m. coraco-brachialis caudalis (Clarke 2004). A deep capital incision separates the ventral tubercle from the caudally convex humeral head. The dorsal pneumotricipital fossa is shallow and subtriangular, not containing a pneumatic foramen; this fossa may be for the attachment of m. humerotriceps (Baumel and Witmer 1993). The caudal surface of the deltopectoral crest is concave proximally. The straight distal margin of the humerus is nearly perpendicular to the shaft, without a well-developed flexor process commonly present in enantiornithines. Neither tricipital grooves nor an olecranon fossa is developed (Figure 8).

The left ulna is preserved in ventral view in GSGM-07-CM-006 (Figure 7); the left ulna in GSGM-05-CM-014 is exposed ventrally and the right element is in dorsal view (Figure 8). Compared with the radius, the ulna is slightly more curved but not bowed proximally as in most other ornithothoracines. Proximally, the intercotylar crest is distinct and slightly broad, dividing the two cotylae. The ventral cotyla is larger and more concave than the dorsal one. The olecranon process is low and rounded (Figure 7). A narrow, shallow longitudinal groove is present on the ventral surface of the ulnar shaft (Figure 8); remige papillae are not visible.

The radii in GSGM-07-CM-006 and GSGM-05-CM-014 are all exposed in caudal view. The radius is very slightly S-shaped caused by a slight deflection of the distal end, and is more than half the width of the ulna. The humeral cotyla is nearly round and proximally flat (Figure 7). A bicipital tubercle is present on the proximal ventral surface, similar to that in *Ichthyornis* (CAGS-IG-04-CM-004; You et al. 2006). However, this tubercle in *Gansus* is located distally to a triangular, relatively smooth and well demarcated fossa (CAGS-IG-04-CM-004; You et al. 2006), whereas in *Ichthyornis* the bicipital tubercle as well as a narrow-angling ridge are present distally to a less demarcated region (Clarke 2004). The distal end is expanded craniocaudally, and its caudodistal tip is slightly hooked proximally (Figure 7). A shallow impression is present on the cranial surface of the distal end. The articular surface of the distal end is slightly convex (Figure 8).

The ulnare and radiale are equal in size (Figure 7). The ulnare is heart-shaped, with a shallow metacarpal incisure. The short dorsal ramus bears a shallow, round fossa. The relatively elongated ventral ramus bears a tendinal groove, which is shallower than that of *Ichthyornis* (Clarke 2004), but situated nearly in the same position. The radiale has two major articular facets (carpal and radial). However, due to the limitation of materials, the detailed morphology of the radiale is difficult to be compared with other ornithuromorphs.

The preserved carpometacarpi in GSGM-07-CM-006 and GSGM-05-CM-014 are both in ventral view. The supratrochlear fossa on the proximodorsal surface is slightly concave. A well-developed pisiform process forms a peg-like ventral projection (Figure 7(C)), similar to that of *Apsaravis* and *Yixianornis* (Clarke and Norell 2002; Clarke et al. 2006). The major and minor metacarpal are fused proximally and distally, and approximately equal in distal extent. The intermetacarpal space is nearly as wide as the minor metacarpal. This space is distally restricted, not reaching the distal articular surface of the alular metacarpal. An intermetacarpal process is absent. The distal end of the ventral surface of the carpometacarpus is relatively smooth, without any tubercle or scars, which are present in *Ichthyornis* (Clarke 2004)

The manual phalanges are preserved in GSGM-05-CM-014 (Figure 8). The first phalanx of the alular digit is bowed, and slightly shorter than half the length of the carpometacarpus. The alular digit ungual is slightly longer than that of the major digit (Table 1). The first phalanx of the major digit is robust and craniocaudally expanded to nearly twice the width of the major metacarpal (You et al. 2006), as in other ornithuromorphs. The intermediate phalanx is unmodified, more slender and bowed than the first; its distal articulation with the ungual appears to be ginglymous (CAGS-IG-04-CM-004; You et al. 2006). The two major digit non-ungual phalanges are approximately equal in length, and both bear a flange-like process in their middle region, respectively. The major digit ungual has a small flexor tubercle. The minor digit retains only one phalanx, which possesses a relatively large, flange-like caudal expansion almost half way from the proximal end; it is tapered to the distal end and approximately twice as long as the major digit ungual, similar to that of *G. zheni* and *Iteravis* (Figure 8; Liu et al. 2014; Zhou, O'Connor, et al. 2014).

Pelvic girdle

The right ilium is preserved in its entirety in GSGM-07-CM-009. The preacetabular wing of the ilium extends cranially over the synsacrum, reaching the second cranialmost thoracic vertebra (Figure 2). The cranial margin of the ilium is nearly rounded, and the tapered caudal end surpasses the distal end of the synsacrum. The preacetabular wing of the ilium is shorter than the postacetabular wing, similar to *Iteravis* (Zhou, O'Connor, et al. 2014). The acetabulum is relatively large, with a laterally projected antitrochanter on the caudodorsal margin. Compared with other basal ornithuromophs, the ilium of *Gansus yumenensis* is relatively slender (dorsoventrally narrow), resembles that of some extant aquatic birds.

The ischium extends further distally than the caudal end of the ilium (Figure 2). A dorsal process is present near the midpoint of the ischium as in CAGS-IG-04-CM-002 (You et al. 2006); the process is large and obtusely

Table 1. Selected measurements (mm) of five specimens of *Gansus yumenensis*.

Element and dimension	07-CM-006	05-CM-014	07-CM-009	04-CM-018	07-CM-011
Scapula					
Coracoid	21.6[e]				
Coracoid distal width					
Furcula					
Furcula width (maximum)					
Humerus	49.7	47.8			
Ulna	54.3	51.1			
Radius	52.8	48.9			
Carpometacarpus		23.7			
Major metacarpal width		1.4			
Minor metacarpal width		0.7			
Alular digit 1		9.6			
Alular digit 2		3.6[e]			
Major digit 1					
Major digit 2					
Major digit 3		2.8			
Minor digit 1		5.8			
Ilium			37.9		
Ischium			24.2		24.4
Pubis					47.7
Femur		29.3			30.2
Tibiotarsus (not including cnemial crest)		63.7		61.0	61.5
Cnemial crest		3.7		3.8	4.5
Tarsometatarsus		40.0			37.9
Pedal digit I-1		7.3			8.3
Pedal digit I-2		4.1			3.5
Pedal digit II-1		15.1			12.5
Pedal digit II-2		12.9			12.4
Pedal digit II-3		4.6			4.6
Pedal digit III-1		13.5			14.1
Pedal digit III-2		12.2			9.4
Pedal digit III-3		9.0			8.6
Pedal digit III-4		4.6			3.1
Pedal digit IV-1		12.0			11.0
Pedal digit IV-2		9.7			8.9
Pedal digit IV-3		8.7			7.6
Pedal digit IV-4		9.3			8.6
Pedal digit IV-5		3.7			3.4

[e] Estimated value.

triangular, similar to *Changmaornis*, *Yanornis*, *Schizooura* and *Iteravis* and most resembling that of *Yixianornis* (Zhou and Zhang 2001; Clarke et al. 2006; Zhou et al. 2012; Wang et al. 2013). In contrast, a dorsal process is absent in *Longicrusavis*, *Archaeorhynchus* and *Hongshanornis* (Zhou and Zhang 2005, 2006; O'Connor et al. 2010). *Confuciusornis* has a similar morphology but the dorsal process is much longer and more proximally located on the caudal margin of the ischium (Chiappe et al. 1999) and a second distal process is also present in *Confuciusornis* and *Chaoyangia* (O'Connor and Zhou 2013). A low ridge is developed on the lateral surface of the ischium, extending from the acetabulum to the midpoint of the shaft, similar to *Yixianornis* and *Iteravis*; however, in *Yixianornis* and *Iteravis* the ridge extends along the entire

length of the ischium. The caudal part of the ischium tapers to its terminus, as in *Changmaornis, Yixianornis* and *Iteravis*. The shaft of the ischium is neither fused nor in contact with the ilium; consequently, an ilioischiadic foramen is absent, contrary to You et al. (2006).

The pubis is longer than the ilium (Table 1). It is slender and retroverted so that it is nearly parallel to the ischium (Figure 3), as described in You et al. (2006), but the shaft is not compressed mediolaterally as in *Apsaravis* and *Changmaornis* (Clarke and Norell 2002; Wang et al. 2013). The distal ends of the pubes are unfused but expanded where they are appressed to each other, likely forming a short symphysis (Figure 3), as in CAGS-IG-04-CM-002 (You et al. 2006); the expansions of the pubes are also present in *G. zheni* and *Iteravis* (Liu et al. 2014; Zhou,

Figure 9.   (Colour online) Photographs of *Gansus yumenensis* GSGM-04-CM-018: (A) in caudal view; (B) in cranial view. Abbreviations: cc, cnemial crest; fbh, fibular head; fc, fibular crest; lc, lateral condyle; mc, medial condyle; tu, tubercles.

O'Connor, et al. 2014). In contrast, In contrast, in *Yanornis*, *Jianchangornis* and *Yixianornis*, although the pubic symphysis is developed, the distal expansion is absent.

Hind limb

The femur is short and weakly bowed craniocaudally (Figure 8). Proximally, the femoral head is large and bulbous, with a short and robust neck continuous with the trochanteric crest (Figure 3), as in CAGS-IG-04-CM-002 (You et al. 2006). The pit for the capital ligament on the femoral head is small and shallow. The trochanteric crest is poorly developed, not projecting proximally beyond the femoral head. A posterior trochanter is absent. The femoral shaft bears a marked cranial intermuscular line. The impression of the lateral collateral ligament is shallow.

The astragalus and calcaneum are completely fused to each other and the tibia. The tibiotarsus is long and straight, and just beyond twice the length of the femur (Table 1). The cranial cnemial crest and the lateral crest are conjoined proximally, projecting proximally beyond the articular surface of the tibiotarsus; the cranial surface between the two crests is deeply concave (Figure 9). However, the conjoined cnemial crests in GSGM-05-CM-

014 and -04-CM-018 (Figures 8 and 9) seem more round-shaped, whereas the shapes of the cnemial crests in CAGS-IG-04-CM-002 (You et al. 2006) and IVPP V15080 (Li et al. 2011) are more rectangular; we are unable to determine whether or not this difference is produced by the proximal ends of the cnemial crests in GSGM-05-CM-014 and -04-CM-018 being flattened during diagenesis. The degree of proximal projection of the cnemial crests of *Gansus* is greater than that of other known Early Cretaceous Jehol ornithuromorphs and the Late Cretaceous *Ichthyornis*, but the crests are shorter than those in Hesperornithiformes. The fibular crest is well developed, extending distally along the proximal quarter of the tibiotarsus (Figure 9). Cranially, the extensor canal is poorly developed as a shallow depression, and a supratendinal bridge is absent (You et al. 2006; Figures 8 and 9). However, on the cranial surface proximal to the condyles, the tibiotarsus bears three distinct tubercles, rather than two tubercles in *Changmaornis* and *Apsaravis* (Clarke and Norell 2002; Wang et al. 2013). One is subtriangular and located nearly midway between the condyles. The second tubercle is positioned proximal and lateral to the first. The last is located medially, forming an elongate ridge that runs on the craniomedial margin of the tibiotarsus (Figure 8(C)). The intercondylar incisure separating the medial and lateral condyles is broad and shallow. The lateral condyle is slightly larger and broader than the medial one (Figure 8(C)).

The fibula is very slender, and firmly appressed to the tibiotarsus (Figure 9). Proximally, the fibular head is small and sub-rounded. The articular surface with the femur is concave. The fibular shaft becomes mediolaterally compressed, and extends for more than half the length of the tibiotarsus.

The distal tarsals are completely fused to the metatarsals (Figure 10). The straight tarsometatarsus is longer than the femur and more than half the length of the tibiotarsus. Metatarsals II–IV are also well fused to each other throughout their lengths. Metatarsal V is absent. Proximally, the medial and lateral cotylae are slightly concave (Figure 10(C)). An intercotylar eminence is only weakly developed. A deep dorsal infracotylar fossa excavates the proximodorsal surface. Two tubercles are present in the middle of the deep extensor sulcus (Figure 10(A)), whereas only one tubercle was described by You et al. (2006); based on their positions, they are identified as the attachments for m. tibialis cranialis (Baumel and Witmer 1993), similar to *Ichthyornis* (Clarke 2004). The proximoplantar surface of the tarsometatarsus is projecting plantarly, forming a large prominence that extends for 10% the length of the tarsometatarsus, similar to that in *Changmaornis*, *Yixianornis* and *Yanornis*. This primitive hypotarsus is not developed into distinct crests or sulci, as described in CAGS-IG-04-CM-003 (You et al. 2006). A single, small proximal vascular foramen
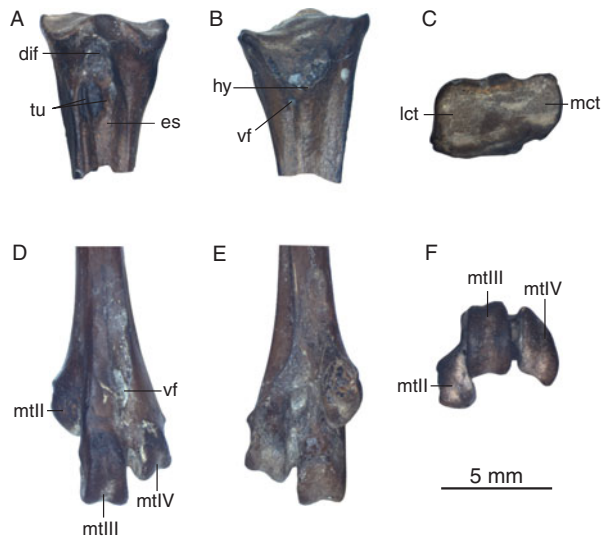
Figure 10. (Colour online) Photographs of *Gansus yumenensis* GSGM-04-CM-031. (A),(D) proximal and distal ends in dorsal view; (B),(E) proximal and distal ends in plantar view; (C) proximal end in proximal view; (F) distal end in distal view. Abbreviations: dif, dorsal infracotylar fossa; es, extensor sulcus; hy, hypotarsus; lct, lateral cotyla; mct, medial cotyla; mt II–IV, metatarsal II–IV; tu, tubercles; vf, vascular foramina.

perforates the tarsometatarsus between metatarsals III and IV just laterodistal to the hypotarsus, which resembles that of *Apsaravis* and *Ichthyornis*.

Metatarsal I is short, articulating on the medioplantar surface of metatarsal II just proximal to the metatarsal II trochlea (Figure 3). The distal end of metatarsal I is nearly perpendicular to the long axis of the metatarsal II, and has a small collateral ligament pit on the medial surface. Metatarsal III is the longest; the proximal end of the shaft is displaced plantarly relative to metatarsals II and IV (Figure 10). Metatarsal IV is slightly shorter than metatarsal III, and metatarsal II is the shortest. The distal condyles of the three metatarsals are not in the same plane; metatarsals II and IV are displaced plantarly, with the former in a greater degree. A collateral ligament pit is present on the lateral and medial surfaces of all the three trochleae. The metatarsal III and IV trochleae are strongly ginglymous, while the trochlea of metatarsal II is only weakly ginglymous, as in *Apsaravis*. The plantar surface of the distal end of the tarsometatarsus is strongly concave, defined medially and laterally by plantar crests.

The pedal phalanges are well preserved in GSGM-07-CM-011 and GSGM-05-CM-014 (Figures 3 and 8). The articular surfaces between all the nonungual phalanges are ginglymoid. Digit IV is the longest among all the digits, and digits III and IV are both longer than tarsometatarsus. The collateral ligament pits are well developed on all the nonungual phalanges. Digit I is reversed and slightly more delicate than the other digits; the first phalanx is

approximately twice as long as metatarsal I and slightly bowed, whereas the flexor tubercle on the ungual phalanx is poorly developed compared with the other digits. The proximal two phalanges of digit II are nearly equal in length although the penultimate phalanx is shorter. Phalanx III-1 is the longest in the foot and much longer than phalanx III-2 and III-3; the length of the phalanges in digit III decrease by approximately 25% (Table 1). The nonungual phalanges of digit IV are slender and shorter than those of other digits; phalanx IV-1 is the longest in this digit, while phalanx IV-4 is slightly shorter than IV-2 and longer than IV-3.

All the unguals are only weakly recurved, suggesting a terrestrial habitat; they bear remarkably pointed flexor tubercles located just proximal to the ventral midpoint, distal to which the ventral surface is concave and the claw is sharply tapered. The unguals are all nearly the same size (Figure 3; Table 1). Shallow grooves are present on the distal portions of both the medial and lateral surfaces. No keratinous ungual sheaths are preserved in any specimen of *Gansus* although these are preserved in some enantiornithines from this locality (O'Connor, Personal Observation).

Gastroliths

Three of the new specimens preserve gastroliths (GSGM-06-CM-011, -07-CM-011 and 05-CM-014) (Figures 3, 6 and 8). Nearly 30 gastroliths are preserved in GSGM-06-CM-011 and 20 in GSGM-07-CM-011. The gastroliths consist of quartz sandstone and sandstone, packed closely together and differing in size and morphology but all strongly polished and weakly rounded. The stones are proportionately larger and fewer than those in *Yanornis* and *Archaeorhynchus* and resemble the gastroliths preserved in *G. zheni* and *Iteravis* in size and morphology (Zhou et al. 2004, 2013; Zhou, O'Connor, et al. 2014; Liu et al. 2014).

Phylogenetic analysis

A phylogenetic analysis was performed using a modified dataset of O'Connor and Zhou (2013), with the addition of *Yumenornis*, *Changmaornis* and *Jiuquanornis* (You et al. 2010; Wang et al. 2013). Thirty-six scorings for *Gansus* were modified based on this study (see Supplementary File). Dromaeosauridae was scored as the outgroup. A matrix of 245 characters (31 ordered; all characters weighted equally) and 61 taxa was analysed using TNT1.1 (Goloboff et al. 2008), applying a heuristic search retaining 10 shortest trees from every 1000 trees followed by an additional round of tree bisection reconnection branch swapping. This analysis produced 1728 most parsimonious trees of 824 steps (CI = 0.393, RI = 0.674).

The strict consensus tree (Figure 11) is consistent with the placements of clades of the non-ornithothoracines in O'Connor and Zhou (2013) and the enantiornithines in O'Connor and Zelenkov (2013), respectively. *Archae-*
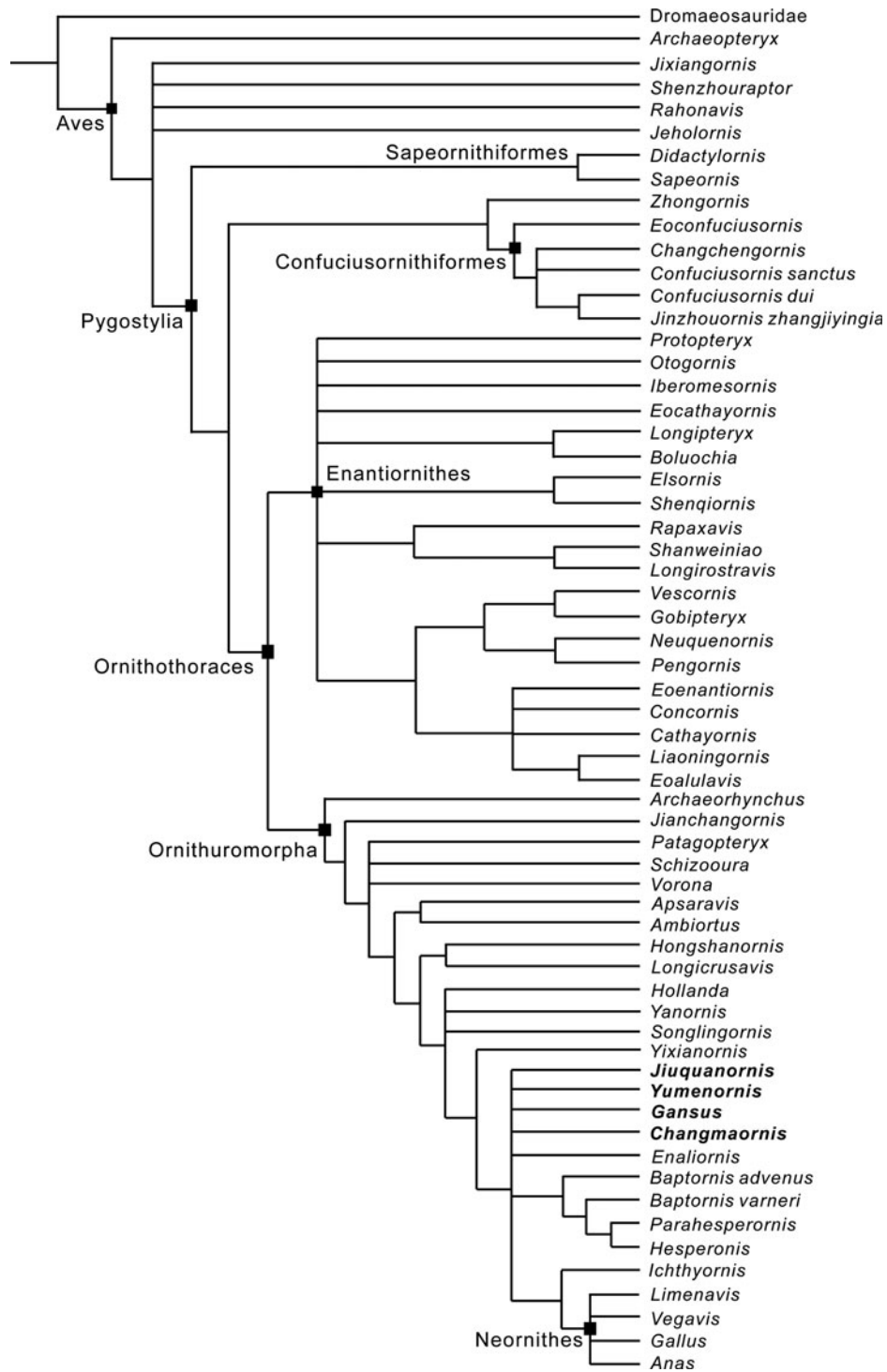
Figure 11. Strict consensus tree illustrating the phylogenetic positions of Changma ornithuromorphs. Tree length: 824 steps, consistency index = 0.393, retention index = 0.674.

orhynchus is resolved as the basalmost ornithuromorph. Within Ornithuromorpha, *Jianchangornis* and *Archaeorhynchus* are resolved as successive outgroups to a polytomy consisting of *Patagopteryx*, *Schizooura*, *Vorona* and a clade including all other derived ornithuromorphs. *Yixianornis* is recovered to be more derived than *Hollanda*, *Yanornis* and *Songlingornis* and as the sister taxon to a large polytomy including *Jiuquanornis*, *Yumenornis*, *Gansus*, *Changmaornis*, *Enaliornis*, the Hesperornithiformes clade and the clade consisting of *Ichthyornis* + Neornithes.

Discussion

This detailed study of seven new specimens and two previously reported specimens of *Gansus yumenensis* reveals new anatomical information for this taxon. Although most features previously described are confirmed (Hou and Liu 1984; You et al. 2006; Li et al. 2011), some are revised, including the presence of the uncinate processes and gastroliths, the absence of an ilioischiadic foramen and the presence of two tubercles in the extensor sulcus of metatarsal III. New important anatomical details include the absence of an n. supracoracoideus foramen on the coracoid, a long acromion process on the scapula and a rounded rostral margin, angled craniolateral processes, rounded lateral processes, medially curved lateral trabeculae and medial fenestrae on the sternum. The sternal morphology is similar to those of *Yumenornis* also from Changma, and *Yanornis*, *Yixianornis* and *Songlingornis* from Jehol Group, although differing in details such as the shape of the lateral process, lateral trabeculae and medial fenestrae (Figure 12). This similarity may suggest a convergent evolution among the taxa from different time and places towards an optimal sternal morphology. A similar morphology is also observed in some living birds (e.g., Columbidae, *Sclererurus*, *Grallaricula*, *Conopophaga*).

In *Gansus yumenensis*, the forelimb is slightly shorter than the hind limb. The ratio of the total forelimb (humerus + ulna + carpometacarpus) to hind limb (femur + tibiotarsus + tarsometatarsus) length is about 0.91 (Table 2), larger than that of *Longicrusavis* and other hongshanornithids, but smaller than most basal Early

Cretaceous ornithuromorphs, including *Archaeorhynchus*, *Jianchangornis*, *Yixianornis*, *Yanornis*, *G. zheni* and *Iteravis*. The femur of *Gansus* is described as shorter than both the tibiotarsus and tarsometatarsus; however, the femur lengths observed in a larger sample of *Gansus yumenensis* specimens are discovered to fall into two groups: in some specimens, the femur is shorter than half the length of the tibiotarsus and shorter than the tarsometatarsus (CAGS-IG-04-CM-002, GSGM-05-CM-014, -07-CM-011; Table 2), whereas others are longer than half the length of the tibiotarsus and only slightly shorter or even longer than the tarsometatarsus (IVPP V15080, V15084; Table 2; Li et al. 2011; Nudds et al. 2013). Whether this variation is inter- or intraspecific is difficult to determine because of the incomplete nature of most of the fossils and remains to be further studied.

The large number of gastroliths preserved in the abominable region in the three new specimens may suggest an herbivorous diet for *Gansus yumenensis*, as has been inferred for other ornithuromorphs preserving gastroliths (Zheng et al. 2011; Zhou et al. 2013). However, the absence of preserved skull material and direct dietary clues prevent us from further interpreting the diet of this taxon.

Gansus yumenensis was first resolved as a member of Ornithurae more derived than all known ornithuromorphs from the Jehol Group of northeastern China and closely related to *Ichthyornis* and the Hesperornithiformes (You et al. 2006). However, with the discovery of new specimens, *Gansus yumenensis* has been revealed to be a more basal ornithuromorph taxon falling outside Ornithurae (O'Connor
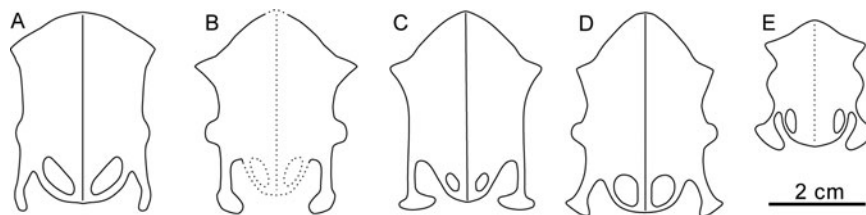

Figure 12. Comparison of the sternum of *Gansus yumenensisi* (A) with other Early Cretaceous ornithuromorphs. (B) *Yumenornis huangi*. (C) *Yanornis martini*. (D) *Yixianornis grabaui*. (E) *Songlingornis linghensis*. Dashed lines in (B) and (E) represent estimated characters. Source: Modified from Wang et al. (2013).

Table 2. Limb bone proportions of selected elements of *Gansus yumenensis*.

Specimen number	Humerus/ulna	Femur/tibiotarsus	Femur/tarsometatarsus	Forelimb/hind limb
GSGM-05-CM-014		0.46	0.73	0.91
GSGM-07-CM-006	0.92			
GSGM-07-CM-011		0.49	0.80	
CAGS-IG-04-CM-002		0.46		
CAGS-IG-04-CM-003	0.92			
CAGS-IG-04-CM-004	0.98			
IVPP V15080		0.56	1.05	
IVPP V15084		0.75	0.86	

et al. 2011; O'Connor and Zhou 2013). In the phylogenetic analysis presented here we updated the scorings of *Gansus yumenensis* based on the new specimens and added three other Changma ornithuromorphs. The results place all four Changma ornithuromorphs in a polytomy with more derived birds (*Enaliornis*, Hesperornithiformes and *Ichthyornis* + Neornithes); this node is supported by seven synapomorphies: a synsacrum formed by 10 ankylosed sacral vertebrae (character 64: $3 \rightarrow 4$); gastralia absent (character 81: $0 \rightarrow 1$); costal facets on the sternum present (character 116: $0 \rightarrow 1$); pisiform process present (character 156: $1 \rightarrow 2$); alular digit short (character 168: $1 \rightarrow 2$); intercotylar eminence present (character 228: $0 \rightarrow 1$) and metatarsal II trochlea strongly displaced plantarly with respect to III and IV (character 237: $0 \rightarrow 2$). Although the interrelationships among Changma ornithuromorphs remain vague, they are all resolved in a position more derived than the Jehol ornithuromorphs. The relatively more derived position of all the known ornithuromorphs is also consistent with the fact that there are no basal birds (e.g., basal pygostylians Sapeornithiformes and Confuciusornithiformes) in the Changma avifauna. Considering the geographic variation, the difference between Changma and Jehol avifaunas may be due to different climate conditions and environment. But we hope further research on stratigraphy and paleoecology would help us better understand the origin of this discrepancy.

Disclosure statement

No potential conflict of interest was reported by the authors.

Supplemental data

The revised character states for *Gansus yumenensis* used in the phylogenetic analysis in this study can be accessed here: http://dx.doi.org/10.1080/08912963.2015.1006217.

References

Baumel JJ, Witmer LM. 1993. Osteologia. In: Baumel JJ, King AS, Breazile JE, Evans HE, Berge JCV, editors. Handbook of avian anatomy: nomina anatomica avium. 2nd ed. Cambridge (MA): Nuttall Ornithological Club; p. 45–132.

Chiappe LM. 2002. basal bird phylogeny: problems and solutions. In: Chiappe LM, Witmer LM, editors. Mesozoic birds: above the heads of Dinosaurs. Berkeley: University of California Press; p. 448–472.

Chiappe LM, Calvo JO. 1994. *Neuquenornis volans*, a new Late Cretaceous bird (Enantiornithes: Avisauridae) from Patagonia, Argentina. J Vert Paleontol. 14(2):230–246. doi:10.1080/02724634.1994.10011554.

Chiappe LM, Ji S, Ji Q, Norell MA. 1999. Anatomy and systematics of the Confuciusornithidae (Theropoda: Aves) from the Late Mesozoic of northeastern China. Bull Am Mus Nat Hist. 242:1–89.

Clarke JA. 2004. Morphology, phylogenetic taxonomy, and systematics of *Ichthyornis* and *Apatornis* (Avialae: Ornithurae). Bull Am Mus Nat Hist. 286:1–179.

Clarke JA, Norell MA. 2002. The morphology and phylogenetic position of *Apsaravis ukhaana* from the Late Cretaceous of Mongolia. Am Mus Novit. 3387:1–46.

Clarke JA, Zhou Z, Zhang F. 2006. Insight into the evolution of avian flight from a new clade of Early Cretaceous ornithurines from China and the morphology of *Yixianornis grabaui*. J Vert Paleontol. 208:287–308.

Goloboff PA, Farris JS, Nixon KC. 2008. TNT, a free program for phylogenetic analysis. Cladistics. 24(5):774–786. doi:10.1111/j.1096-0031.2008.00217.x.

Harris JD, Lamanna MC, You H, Ji S, Ji Q. 2006. A second enantiornithean (Aves: Ornithothoraces) wing from the Early Cretaceous Xiagou Formation near Changma, Gansu Province, People's Republic of China. Can J Earth Sci. 43(5):547–554. doi:10.1139/e06-007.

Hou L. 1997. Mesozoic birds of China. Nantou: Feng-Huang-Ku Bird Park of Taiwan Provincial Government.

Hou L, Liu Z. 1984. A new fossil bird from Lower Cretaceous of Gansu and early evolution of birds. Sci Sin Ser B. 27:1296–1301.

Ji S, Atterholt J, O'Connor JK, Lamanna MC, Harris JD, Li D, You H, Dodson P. 2011. A new, three-dimensionally preserved enantiornithine bird (Aves: Ornithothoraces) from Gansu Province, northwestern China. Zool J Linnean Soc. 162(1):201–219. doi:10.1111/j.1096-3642.2010.00671.x.

Kurochkin YN. 1982. New order of birds from the Lower Cretaceous in Mongolia. Paleontology. 262:452–455.

Lamanna MC, Li D, Harris JD, Atterholt J, You H. 2006. Exceptionally-preserved Enantiornithes (Aves: Ornithothoraces) from the Early Cretaceous of northwestern China. Acta Palaeontol Pol. 51(3):423–434.

Li Y, Zhang Y, Zhou Z, Li Z, Liu D, Wang X. 2011. New material of *Gansus* and a discussion on its habit. Vertebr Palasiat. 49:435–445 (in Chinese).

Linnaeus C. 1758. Systems naturae. 10th ed. Laurentii Salvii: Holmiae.

Liu D, Chiappe LM, Zhang Y, Bell A, Meng Q, Ji Q, Wang X. 2014. An advanced, new long-legged bird from the Early Cretaceous of the Jehol Group (northeastern China): insights into the temporal divergence of modern birds. Zootaxa. 3884(3): 253–266. http://dx.doi.org/10.11646/zootaxa.3884.3.4.

Nudds RL, Atterholt J, Wang X, You H, Dyke GJ. 2013. Locomotory abilities and habitat of the cretaceous bird *Gansus yumenensis* inferred from limb length proportions. J Evol Biol. 26(1):150–154. doi:10.1111/jeb.12036.

O'Connor JK, Chiappe LM, Bell A. 2011. Pre-modern birds: avian divergences in the Mesozoic. In: Dyke GD, Kaiser G, editors. Living Dinosaurs: the evolutionary history of birds. Hoboken (NJ): John Wiley & Sons; p. 39–114.

O'Connor JK, Gao KQ, Chiappe LM. 2010. A new ornithuromorph (Aves: Ornithothoraces) bird from the Jehol Group indicative of higher-level diversity. J Vert Paleontol. 30(2):311–321. doi:10.1080/02724631003617498.

O'Connor JK, Zelenkov NV. 2013. The phylogenetic position of *Ambiortus*: comparison with other Mesozoic birds from Asia. Paleontol J. 47(11):1270–1281. doi:10.1134/S0031030113110063.

O'Connor JK, Zhou Z. 2013. A redescription of Chaoyangia beishanensis (Aves) and a comprehensive phylogeny of Mesozoic birds. J Syst Palaeontol. 11(7):889–906. doi:10.1080/14772019.2012.690455.

Suarez BM, Ludvigson AG, González AL, Al-Suwaidi HA, You H. 2013. Stable isotope chemostratigraphy in lacustrine strata of the Xiagou Formation, Gansu Province, NW China. In: Bojar AV, Melinte-Dobrinescu MC, Smit J, editors. Isotopic studies in Cretaceous research geological society. Special Publications, 382. Bath: The Geological Society Publishing House; p. 143–156.

Wang Y, O'Connor JK, Li D, You H. 2013. Previously unrecognized Ornithuromorph bird diversity in the Early Cretaceous Changma Basin, Gansu Province, Northwestern China. PLoS ONE. 8(10): e77693. doi:10.1371/journal.pone.0077693.

You H, Atterholt J, O'Connor JK, Harris JD, Lamanna MC, Li D. 2010. A second Cretaceous Ornithuromorph bird from the Changma Basin, Gansu Province, Northwestern China. Acta Palaeontol Pol. 55(4): 617–625. doi:10.4202/app.2009.0095.

You H, O'Connor JK, Chiappe LM, Ji Q. 2005. A new fossil bird from the Early Cretaceous of Gansu Province, northwestern China. Hist Biol. 17(1–4):7–14. doi:10.1080/08912960500284851.

You H, Lamanna MC, Harris JD, Chiappe LM, O'Connor JK, Ji S, Lü J, Yuan C, Li D, Zhang X, et al. 2006. A nearly modern amphibious bird from the Early Cretaceous of Northwestern China. Science. 312(5780):1640–1643. doi:10.1126/science.1126377.

Zheng X, Martin LD, Zhou Z, Burnham DA, Zhang F, Miao D. 2011. Fossil evidence of avian crops from the Early Cretaceous of China. PNAS. 108(38):15904–15907. doi:10.1073/pnas.11126 94108.

Zhou Z, Clarke JA, Zhang F, Wings O. 2004. Gastroliths in *Yanornis*: an indication of the earliest radical diet-switching and gizzard plasticity in the lineage leading to living birds? Naturwissenschaften. 91(12): 571–574. doi:10.1007/s00114-004-0567-z.

Zhou Z, Zhang F. 2001. Two new ornithurine birds from the Early Cretaceous of western Liaoning, China. Chin Sci Bull. 46:1–7.

Zhou Z, Zhang F. 2005. Discovery of an ornithurine bird and its implication for Early Cretaceous avian radiation. PNAS. 102(52): 18998–19002. doi:10.1073/pnas.0507106102.

Zhou Z, Zhang F. 2006. A beaked basal ornithurine bird (Aves, Ornithurae) from the Lower Cretaceous of China. Zool Scripta. 35(4):363–373. doi:10.1111/j.1463-6409.2006.00234.x.

Zhou Z, Zhang F, Li Z. 2009. A new basal ornithurine bird (Jianchangornis microdonta gen. et sp. nov.) from the lower Cretaceous of China. Vertebr Palasiat. 47:299–310.

Zhou S, Zhou Z, O'Connor JK. 2012. A new toothless ornithurine bird (*Schizooura lii* gen. et sp. nov.) from the Lower Cretaceous of China. Vertebr Palasiat. 50:9–24.

Zhou S, O'Connor JK, Wang M. 2014. A new species from an ornithuromorph (Aves: Ornithothoraces) dominated locality of the Jehol Biota. Chin Sci Bull. 59(36):5366–5378. doi:10.1007/s11434-014-0669-8.

Zhou S, Zhou Z, O'Connor JK. 2013. Anatomy of the basal ornithuromorph bird *Archaeorhynchus spathula* from the Early Cretaceous of Liaoning, China. J Vert Paleontol. 33(1):141–152. doi:10.1080/02724634.2012.714431.

Zhou S, Zhou Z, O'Connor JK. 2014. A new piscivorous ornithuromorph from the Jehol Biota. Hist Biol. 26(5):608–618. doi:10.1080/08912963.2013.819504.